

Article

Not peer-reviewed version

Rainfall Variability in the Brazilian Subtropical Climate Associated with El Niño–Southern Oscillation Diversity

[Gabriela Goudard](#)*, [Leila Limberger](#), [Camila Bertoletti Carpenedo](#), Francisco Mendonça

Posted Date: 3 March 2026

doi: 10.20944/preprints202603.0167.v1

Keywords: climate variability; ENSO types; precipitation anomalies; Southern Brazil



Preprints.org is a free multidisciplinary platform providing preprint service that is dedicated to making early versions of research outputs permanently available and citable. Preprints posted at Preprints.org appear in Web of Science, Crossref, Google Scholar, Scilit, Europe PMC.

Copyright: This open access article is published under a [Creative Commons CC BY 4.0 license](#), which permit the free download, distribution, and reuse, provided that the author and preprint are cited in any reuse.

Disclaimer/Publisher's Note: The statements, opinions, and data contained in all publications are solely those of the individual author(s) and contributor(s) and not of MDPI and/or the editor(s). MDPI and/or the editor(s) disclaim responsibility for any injury to people or property resulting from any ideas, methods, instructions, or products referred to in the content.

Article

Rainfall Variability in the Brazilian Subtropical Climate Associated with El Niño–Southern Oscillation Diversity

Gabriela Goudard ^{1,2,*}, Leila Limberger ³, Camila Bertolotti Carpenedo ⁴ and Francisco Mendonça ²

¹ Climatology and Environmental Studies Laboratory (CLIMAS), Department of Geography, Federal University of Ceará (UFC), Fortaleza, Brazil

² Climatology Laboratory (LABOCLIMA), Department of Geography, Federal University of Paraná (UFPR), Curitiba, Brazil

³ Environmental Dynamics Study Laboratory (LEDA), Department of Geography, Western Paraná State University (UNIOESTE), Marechal Cândido Rondon, Brazil

⁴ Center for Studies on Climate Change and Variability (NUVEM), Department of Soils and Agricultural Engineering, Federal University of Paraná (UFPR), Curitiba, Brazil

* Correspondence: gabriela.goudard@ufc.br

Abstract

The El Niño–Southern Oscillation (ENSO) is the main driver of interannual climate variability, strongly influencing precipitation, temperature, and extreme events worldwide. In South America, its impacts are well documented. However, studies examining different ENSO types—Eastern Pacific (EP), Central Pacific (CP), and Mixed (MX), defined according to the location of sea surface temperature (SST) anomalies in the tropical Pacific—remain limited, particularly for the Brazilian subtropical climate. This study investigates rainfall variability in the Brazilian subtropical region associated with different ENSO types. Composite analyses of precipitation, wind, and SST anomalies were performed, and monthly rainfall data from 703 stations were used to identify homogeneous regions. The results show the intensity and spatial coherence of rainfall anomalies vary according to El Niño type, with EP events favoring widespread wet conditions and CP events producing more heterogeneous or locally negative anomalies. For La Niña, the intensity and seasonal distribution of negative rainfall anomalies vary by ENSO type: stronger impacts occur in summer (EP), spring (MX), and autumn (CP). These findings improve the understanding of ENSO-related rainfall variability in the Brazilian subtropical region and provide valuable insights for the management of climate-related risks in a region frequently affected by rainfall extremes.

Keywords: climate variability; ENSO types; precipitation anomalies; Southern Brazil

1. Introduction

The El Niño–Southern Oscillation (ENSO) is one of the main drivers of interannual global climate variability, influencing patterns of precipitation and extreme events in different regions of the planet [1–5]. ENSO arises from ocean–atmosphere interactions in the East-Central Equatorial Pacific, where anomalies in sea surface temperature are accompanied by modifications in the zonal pressure gradient and trade wind intensity.

Several scientific studies that highlight the spatio-temporal variability of this phenomenon in different regions of the world [5]. In South America (SA), the warm (cold) phase, called El Niño – EN (La Niña – LN), is characterized by warmer (colder) than usual sea surface temperature (SST) in the East-Central Equatorial Pacific, altering atmospheric and oceanic processes and climatological variables over the continent. The subtropical climate present in southern Brazil and adopted as the

study area in this investigation (Figure 1), is characterized by regular precipitation throughout the year (Figure 4; [6]), with a continuous supply of moisture from the Atlantic Ocean, the Amazon region, and frontal systems [7,8,14]

The main modulators of rainfall in this area are the South American Low-Level Jet (SALLJ) and frontal systems [5,7]. Mesoscale convective systems and frontal systems are the most important rain-producing weather systems in this region, during spring/summer and fall/winter, respectively [6–9]. This region is strongly impacted by positive and negative precipitation anomalies associated with ENSO events, being one of the most sensitive regions in SA to these teleconnections, as highlighted by several studies [6,10–14].

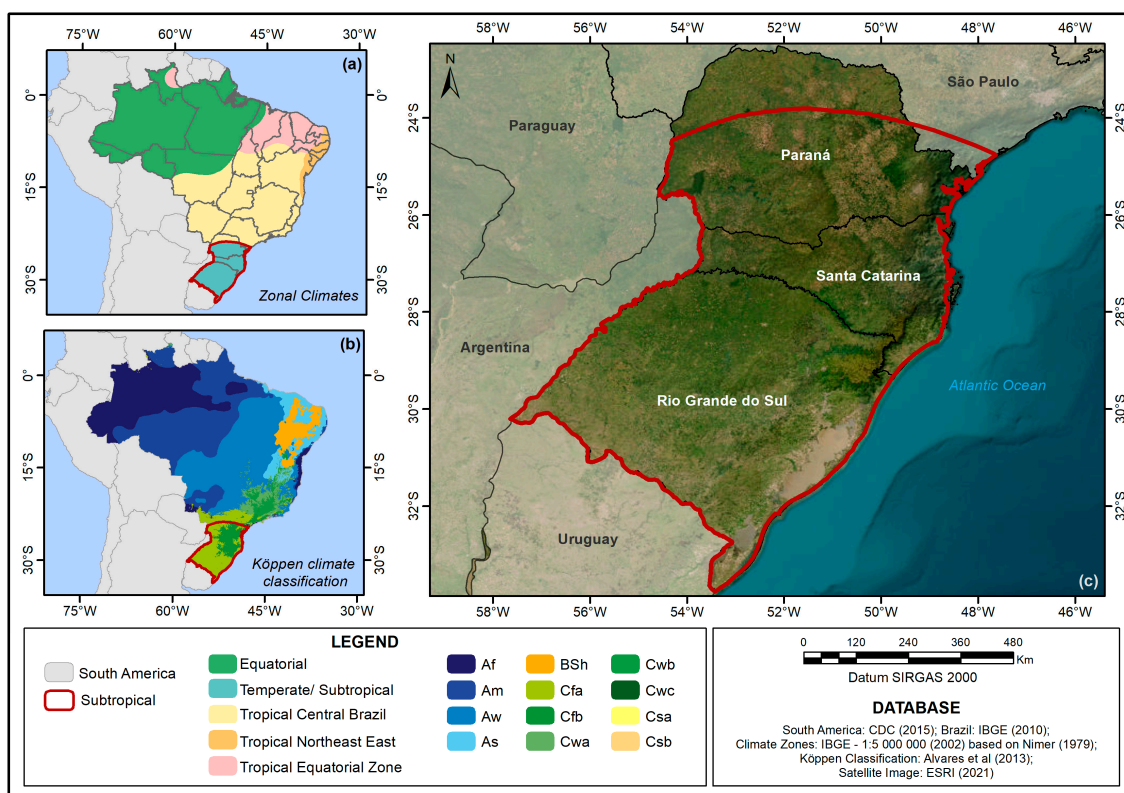


Figure 1. Location and climatic characterization of the Brazilian subtropical climate. (a) Climate Zones – Nimer (1979), (b) Köppen climate classification – Alvares *et al.* (2013), (c) Brazilian subtropical climate and southern states of Brazil.

In general, in this area (Figure 1), during EN (LN) years, precipitation is above (below) climatological averages, with impacts on flood (drought) events. Furthermore, the study area has been impacted by intense rainfall anomalies in recent years, such as the 2020/2021 droughts in various parts of southern Brazil [15,16] and the 2024 floods in the state of Rio Grande do Sul [17]. These scenarios corroborate evidence of increasing extreme events worldwide and in Brazil [18,19]. Therefore, a better understanding of rainfall patterns is necessary in the Brazilian subtropical climate, especially in relation to ENSO, the main mode of interannual variability in the SA.

Even though ENSO events are widely studied, the phenomenon is highly complex. Previous studies have associated the complexity of the ENSO events with its intensity, spatial pattern, temporal evolution, and the combination of these factors [20]. In terms of intensity, ENSO events can be classified as weak, moderate, and strong based on SST anomalies [2]. Recent investigations have highlighted seasonal variations in ENSO intensity, associated with changes in the Walker circulation, Rossby waves propagation and, consequently, precipitation patterns in different SA regions [21].

The spatial pattern differentiates them into Eastern Pacific (EP), Central Pacific (CP), and Mixed (MX) events, according to the areas of maximum SST anomalies, which occur in Niño 3, Niño 4, and

between the Niño 3 and Niño 4 regions, respectively [5,14,22–25]. Furthermore, their temporal evolution or duration divides ENSO events into one-year events and multi-year events (two or three years) [26], which can be cyclical or episodic, depending on their transition [27,28].

In recent decades, the comprehension of the complexity of these ENSO patterns has been intensified by the increased occurrence of multiyear LN and CP-type EN [29]. In addition, the frequency and intensity of EN events are projected to increase due to global warming [30].

Most studies consider the entire South American domain [13,31,32,5,21,33; among others, which limits detailed analyses of Brazilian regions. Previous analyses for southeastern SA demonstrated that EP and CP El Niño events produce distinct rainfall responses due to differences in large-scale circulation patterns [14]. However, regional-scale investigations focusing specifically on the Brazilian subtropical climate remain limited. Thus, the main objective of this paper is to analyze the rainfall variability in the Brazilian subtropical climate associated with ENSO diversity (EP, CP, and MX), also considering homogeneous rainfall regions in the study area.

The present study advances by focusing specifically on the Brazilian subtropical climate, incorporating both EN and LN typologies and applying a rainfall regionalization. Thus, we provide a refined regional-scale assessment of ENSO diversity impacts that has not yet been addressed for this climatic domain. The results contribute to the understanding of seasonal variability of precipitation in the subtropical climate associated with ENSO typologies, as well to improve the management of climate-related risks in an area that has been frequently impacted by both positive and negative rainfall extremes.

2. Materials and Methods

2.1. Database

To characterize precipitation variability in homogeneous regions, monthly data from 703 stations were used (Figure 2), of which 551 are located entirely within the Brazilian subtropical climate, while 152 are in the transition zone to the tropical climate, allowing spatial sampling of data in different climatic and relief contexts of the study area (Figure 2). These data were obtained from the Hidroweb platform of the National Water Agency (ANA), available at <https://www.snirh.gov.br/hidroweb/serieshistoricas>. Additionally, monthly precipitation data from the *Global Precipitation Climatology Centre* (GPCP), with a horizontal resolution of $0.25^\circ \times 0.25^\circ$ [34], were used to compose the monthly anomalies in different types of ENSO.

Furthermore, Extended Reconstructed Sea Surface Temperature version 5 - ERSSTv5 [35] was used, derived from the International Comprehensive Ocean-Atmosphere Dataset (ICOADS), with a spatial resolution of $2^\circ \times 2^\circ$. We also employed the monthly data of 850-hPa and 200-hPa wind from NCEP/NCAR reanalysis [36] in the atmospheric fields. The analyses were conducted for the period 1976–2019, due to greater consistency of data for the study area [6].

2.2. Correction and Processing of Rainfall Data

Corrections to the monthly rainfall data from the 703 stations of Hidroweb were performed using the NIPALS (Non-linear Iterative Partial Least Squares) algorithm, which was selected for the imputation of missing data in the historical time series. This algorithm is based on principal component analysis and regressions for predicting missing values [37]. Additionally, four homogeneity tests were applied: Pettitt, Standard Normal Homogeneity Test (SNHT), Buishand, and Von Neumann, to ensure data consistency [6].

The definition of homogeneous rainfall zones was based on Ward's method. Initially, the stations used in this research were grouped using the Agglomerative Hierarchical Clustering technique, a multivariate method whose objective is to separate data into groups that are not previously known [38]. This procedure was performed based on Ward's method, using the K-means algorithm.

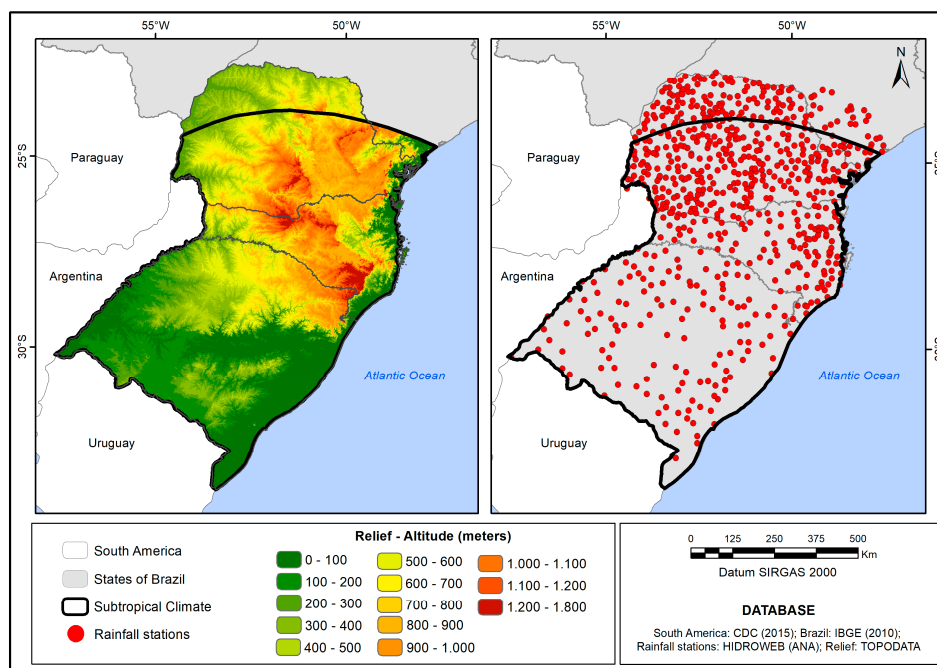


Figure 2. Relief and rainfall stations in the Brazilian subtropical climate.

Rainfall in homogeneous regions was characterized by defining standard years [39] and calculating the coefficient of variation of rainfall. The definition of standard years was carried out to detect extremely dry years (rainfall < the 10th percentile - P10), dry years (P10 to P35), usual years (P35 to P65), rainy years (P65 to P90), and extremely rainy years (> P90).

The annual coefficient of variation (CV) of rainfall was calculated using the equation: $CV = \text{Standard Deviation} / \text{Mean}$. These indices (standard years and coefficient of variation) were used to characterize the different homogeneous rainfall regions of the Brazilian subtropical climate in relation to rainfall patterns in different ENSO typologies.

2.3. Identification of ENSO Events

The determination of ENSO episodes is based on the dates contained in the Oceanic Niño Index – Figure 3a, available at: https://origin.cpc.ncep.noaa.gov/products/analysis_monitoring/ensostuff/ONI_v5.php. ENSO events are selected if they are equal to or greater than $+0.5^{\circ}\text{C}$ (equal to or less than -0.5°C) for the warm phase (cold phase), persistent for 5 consecutive quarters [2].

The characterization of the intensity of the events was based on Golden Gate Weather Services, available at: <https://ggweather.com/enso/oni.htm>. This classification is divided into: weak when SST anomalies ranged from 0.5 to 0.9 (-0.5 to -0.9), moderate from 1.0 to 1.4 (-1.0 to -1.4), strong from 1.5 to 1.9 (-1.5 to -1.9), and very strong when SST anomalies were ≥ 2.0 (≤ -2.0) for EN (LN) events.

In this study, the characterization of events is based on the following procedures [31,32]: EP ENSO occurs with SST anomalies in the adapted Niño 3 region (140°W – 90°W , 5°N – 5°S - with less 10° of longitude on the west side, to obtain separate regions – Figure 3b and Figure 3c) and CP ENSO in the Niño 4 region (160°E – 150°W , 5°N – 5°S ; Figure 3b and Figure 3c).

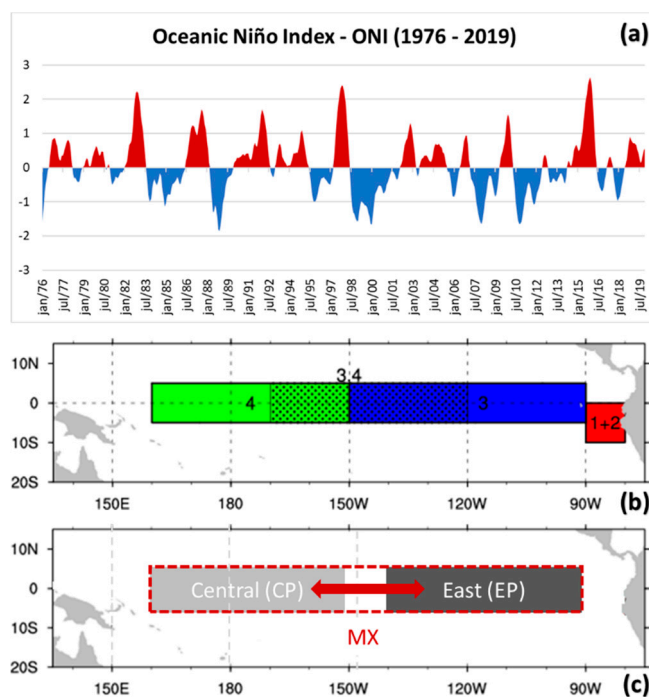


Figure 3. (a) Oceanic Niño Index – ONI (1976 – 2019), (b) Niño regions (NOAA): Niño 1+2 (0°-10°S, 90°W-80°W), Niño 3 (5°N-5°S, 150°W-90°W), Niño 3.4 (5°N-5°S, 170°-120°W), and Niño 4 (5°N-5°S, 160°E-150°W), (c) ENSO regions used in Tedeschi, Grimm and Cavalcanti (2015; 2016) and adapted for this study, including ENSO MX.

MX events were also included in the analysis based on previous studies [14,24,40] (Figure 3c), defined as events that, throughout their space-time evolution (with emphasis on the mature phase of ENSO: DJF), moved between Niño 3 and Niño 4 regions or presented spatial configurations between these two regions (Figure 3c). The separation of LN typologies is more complex compared to EN events, given that the majority present characteristics of overlaps between the Niño 3 and Niño 4 regions.

In the present study, the characterization of ENSO typologies was based on the monthly spatial evolution of SST anomalies during the period of June (year 0) to May (year +1), with emphasis on DJF (Table 1). Following the classification of ENSO events into different typologies, the compositions of SST anomalies in DJF for EP, CP, and MX events were spatially represented. The ENSO typology classification follows the conceptual and methodological framework previously adopted for southeastern SA [14].

2.4. Analysis of Composite Rainfall Anomalies and Statistical Significance Test

We analyzed the composition of seasonal rainfall anomalies from June (year 0) to May (year +1) for years classified for different types of ENSO events (EP, CP, and MX). Additionally, composite analyses of atmospheric anomaly fields were performed, based on 850-hPa and 200-hPa winds. A two-tailed Student's t-test was applied to the composites to determine the areas of statistical significance at the 90% confidence level. The analyses were conducted using the Grid Analysis and Display System (GrADS) software, considering the climatology from 1991 to 2020 for the composition of the anomalies.

3. Results and Discussion

In the Brazilian subtropical climate, annual rainfall varied between 1.100 and 2.600 mm from 1976 to 2019 (Figure 4a). The highest rainfall amounts are recorded in the coastal region of the Paraná State (PR), and between southwestern and western Santa Catarina State (SC). The lowest rainfall

amounts occur in southern Rio Grande do Sul State (RS), with rainfall ranging from 1.100 to 1.300 mm (Figure 4a).

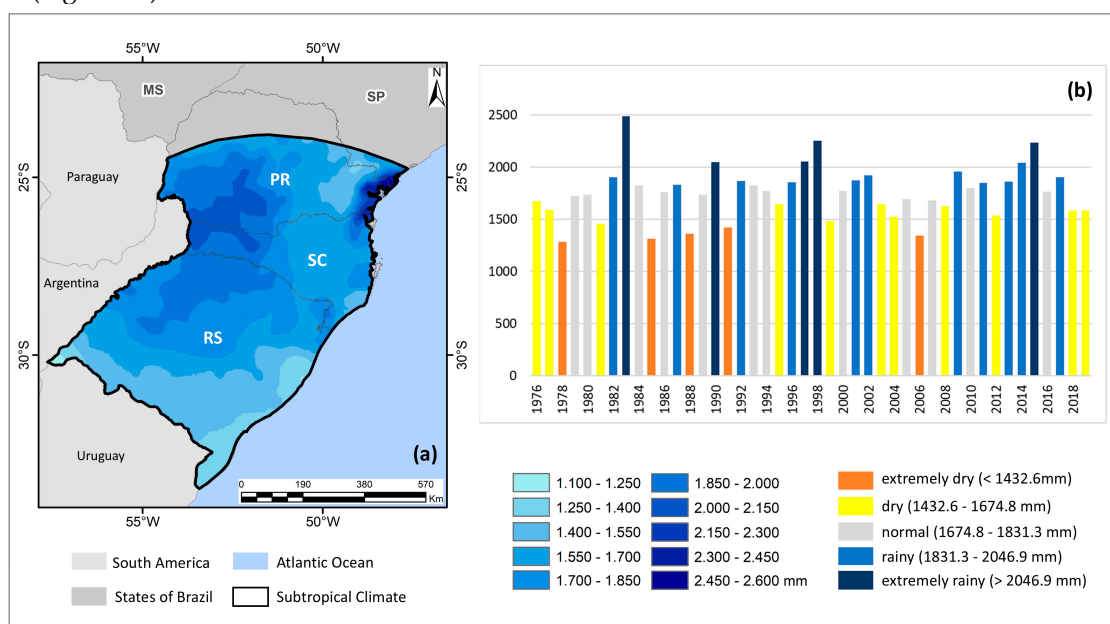


Figure 4. Annual variability of precipitation in the Brazilian subtropical climate (1976 - 2019): (a) spatialization of annual precipitation (mm) and (b) annual precipitation (mm) and classification of standard years.

In relation to seasonal characteristics (not shown), summer and spring have the highest rainfall values, with variations in summer ranging from 250 to 1.100 mm and in spring from 300 to 650 mm on average during the period from 1976 to 2019. In autumn and winter, rainfall is somewhat less significant, with average values ranging from 260 to 700 mm and 150 to 470 mm, respectively. Thus, a certain regularity is observed in the annual and seasonal distribution of rainfall, with lower values only in winter.

The interannual variability of precipitation, characterized by standard years, shows that the years 1978, 1985, 1988, 1991, and 2006 were categorized as extremely dry, while the years 1983, 1990, 1997, 1998, and 2015 were identified as extremely rainy (Figure 4b). The years of very strong EN (such as 1982-1983, 1997-1998, and 2015-2016 – see Table 1) were marked by considerable positive rainfall anomalies in the Brazilian subtropical climate. Some years of the EP La Niña (EPLN), such as 1985 and 2006, presented extremely dry characteristics (Figure 4b and Table 1).

Regarding ENSO events, 30 ENSO episodes were identified in the years 1976 to 2019, of which 16 EN and 14 LN, with different typologies (EP, CP and MX) and intensities (Table 1). Of these events, 7 were categorized as EP (4 EN and 3 LN), 8 as CP (4 EN and 4 LN) and 15 as MX (8 EN and 7 LN). EP events stand out in terms of intensity, with very strong value recorded (Table 1). In terms of frequency of occurrence, MX events stand out (15 events).

Table 1. ENSO events: types in the mature phase (DJF) and intensities (1976 – 2019).

El Niño (EN)	Type (DJF)	Intensity	La Niña (LN)	Type (DJF)	Intensity
1976 – 1977	EP	Weak	1975 - 1976	MX	Strong
1977 – 1978	CP	Weak	1983 - 1984	MX	Weak
1979 - 1980	MX	Weak	1984 - 1985	EP	Weak
1982 - 1983	EP	Very strong	1988 – 1989	MX	Strong
1986 - 1987	MX	Moderate	1995 - 1996	MX	Moderate
1987 - 1988	MX	Strong	1998 – 1999	CP	Strong

1991 - 1992	MX	Strong	1999 - 2000	MX	Strong
1994 - 1995	CP	Moderate	2000 - 2001	CP	Weak
1997 - 1998	EP	Very strong	2005 - 2006	EP	Weak
2002 - 2003	MX	Moderate	2007 - 2008	MX	Strong
2004 - 2005	CP	Weak	2008 - 2009	CP	Weak
2006 - 2007	MX	Weak	2010 - 2011	MX	Strong
2009 - 2010	MX	Moderate	2011 - 2012	CP	Moderate
2014 - 2015	CP	Weak	2017 - 2018	EP	Weak
2015 - 2016	EP	Very strong			
2018 - 2019	MX	Weak			

In EP events (Figures 5a and 5b), maximum SST anomalies occur in the equatorial eastern Pacific (Niño 3 region), occupying a larger extent and being more intense during EN (Figure 5a) than LN (Figure 5b). In MX events (Figures 5c and 5d), the maximum SST anomalies occur concomitantly between the Niño 3 and Niño 4 regions. In contrast to EP events, the MX SST anomalies have a broader meridional extent in LN (Figure 5d) than EN (Figure 5c). For CP events (Figure 5e and Figure 5f), the SST anomalies are in the central Pacific (Niño4 region), being more intense in LN events (Figure 5f).

Composite SST anomalies in the mature phase of ENSO (DJF) highlight a horseshoe or boomerang-shaped pattern noted between the equatorial Pacific SST anomalies inversely with those of the North and South Pacific (Figure 5). This process occurs in all ENSOs, but with a more evident and intense pattern in EP El Niño – EPEN (Figure 5a) and CP La Niña - CPLN (Figure 5f).

Distinct configurations of the Walker circulation observed during EP and CP events arise from the longitudinal displacement of peak SST anomalies in the equatorial Pacific. The shift in maximum SST anomalies causes ascending motions over the tropical Pacific to be more intense and extend over a larger region during EPEN than during CP El Niño - CPEN. In the case of LN years, the descending motion over the Pacific is more intense during CPLN compared to EPLN, conditions highlighted in previous studies [41,42]. These ocean-atmospheric processes interfere with rainfall patterns in the study area, as shown in the analyses developed in this investigation.

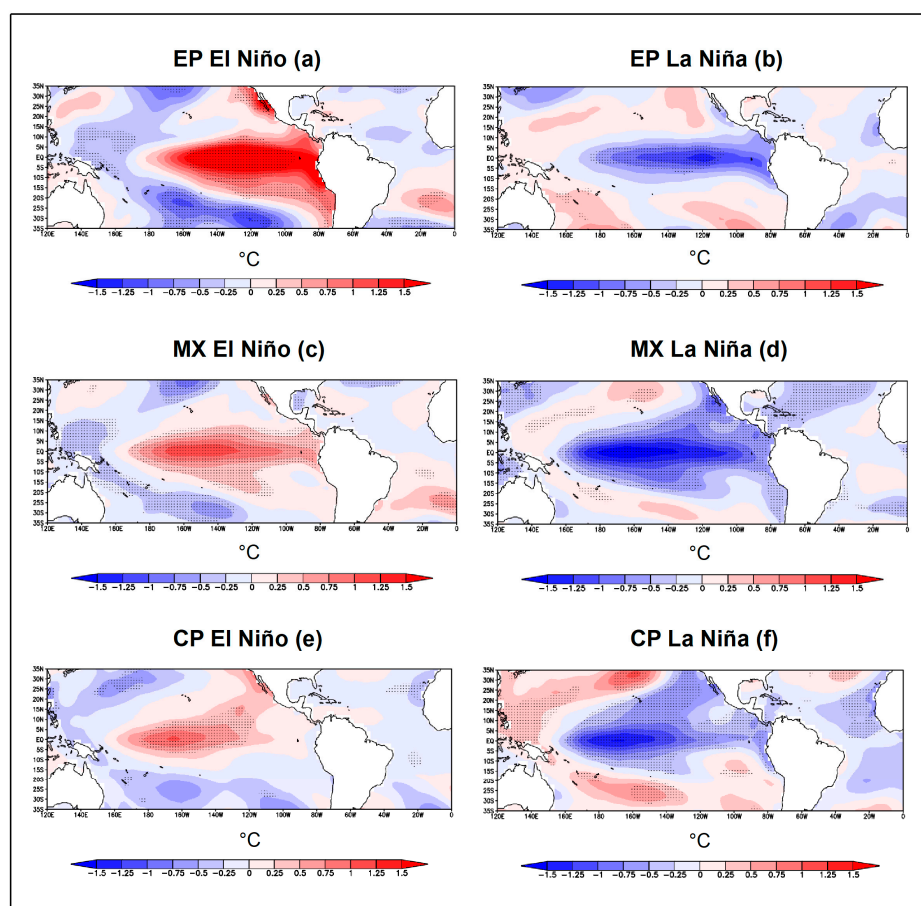


Figure 5. Composites of SST anomalies in DJF (1976 – 2019) for (a) East Pacific El Niño – EP El Niño, (b) East Pacific La Niña – EP La Niña, (c) Mixed El Niño – MX El Niño, (d) Mixed La Niña – MX La Niña, (e) Central Pacific El Niño – CP El Niño and (f) Central Pacific La Niña – CP La Niña (1976 – 2019). Dotted areas are significant at the 90% level based on a two-tailed Student t-test.

Regarding the seasonal rainfall anomaly composites (Figure 6), in EPEN (Table 1 and Figure 6 - first column), positive rainfall anomalies are noted, with increases in rainfall in all seasons of the year, although with few regions showing statistical significance. The spring season (SON0) is the most prominent season of the year, with positive rainfall anomalies throughout the southern region of Brazil (Figure 6d).

In JJA (0), the increases in rainfall are more significant in the state of Paraná and on the southeast coast of Rio Grande do Sul (Figure 6a). In summer (D0JF+1), positive rainfall anomalies are prominent in the southern portion of the study area, particularly in Rio Grande do Sul (Figure 6g). In MAM (+1), the configurations of rainfall anomalies are similar to other seasons of the year, with evidence in the states of Paraná and Santa Catarina (Figure 6j).

Regarding MX El Niño – MXEN (Table 1 and Figure 6 - second column), rainfall decreases are noted on the border between Paraná and Santa Catarina in JJA (0) – Figure 6b. In SON (0), positive anomalies are more expressive in the southwest of the study area, but without statistical significance (Figure 6e). In the summer (D0JF+1), weak negative anomalies are observed in parts of Paraná and Santa Catarina (Figure 6h), and in autumn (Figure 6k), rainfall increases are strong in south-central Paraná and in a large part of Santa Catarina. In MXEN the anomalies are less intense compared to EPEN (Figure 6 – first and second columns).

Seasonal precipitation anomalies for CPEN (Table 1 and Figure 6 - third column) present distinct patterns from those evidenced in EPEN and MXEN, with a predominance of negative rainfall anomalies, but with few areas of statistical significance. The seasons with the greatest variations in rainfall patterns between EPEN and CPEN are D(0)JF(+1) (Figure 6g and Figure 6i) and MAM (+1)

(Figure 6j and Figure 6l). In autumn (MMA+1), negative anomalies predominate throughout the study area, but with statistical significance only in the south of Rio Grande do Sul (Figure 6l), showing a contrary pattern to what occurs in EPEN (Figure 6j) and MXEN (Figure 6k).

The atmospheric mechanisms associated with the different types of ENSO are explored in the 850-hPa vector wind (Figure 7 and supplementary material for winds at 200 hPa). Analyses reveal that the heaviest precipitation in SON (0) in EPEN results from a stronger SALLJ-type circulation (Figure 7d). The enhanced flow along the South Atlantic Convergence Zone (SACZ) region is also intensified in D(0)JF(+1) (Figure 7g). In SON (0) and D(0)JF(+1) (Figures 7d and 7g), the SALLJ-type circulation patterns follow a path slightly positioned north of the climatological circulation, contributing to increased rainfall during this period as well. This pattern is consistent with previous analyses [43]. The strengthening of the SALLJ-type circulation during EP El Niño events observed here is consistent with previous findings for southeastern SA [14].

In MXEN events, a weaker SALLJ-type circulation is observed in JJA (0) (Figure 7b), associated with negative precipitation anomalies over Paraná and Santa Catarina (Figure 6b). Positive precipitation anomalies in the subtropical region predominate during SON (0) – Figure 6e (between southern Paraguay and northeastern Argentina) and MAM (+1) (between Paraná, Santa Catarina, and north-ern Rio Grande do Sul) - Figure 6k. In the southern spring (SON), increased precipitation is associated with the strengthening of the subtropical jet stream (see supplementary material – Figure S1), while in the southern autumn (MAM) there are low-level winds originating in central Brazil (Figure 7k).

On the other hand, in CPEN (Figures 6 and 7 - third column), a weakening of the SALLJ-type circulation is observed, promoting less transport of moisture from the Amazon and the tropical Atlantic, and consequently, the predominance of negative precipitation anomalies for southern Brazil, especially in D(0)JF(+1) and MAM (+1) – Figures 6i and 6l, Figures 7i and 7l).

Analyses at high atmospheric levels (200 hPa - supplementary material - Figure S1) suggest the strengthening of the subtropical jet around 30°S over SA in EPEN, intensifying extratropical cyclones, frontal systems, mesoscale convective systems, and extreme precipitation in the study area, especially in spring and summer. These conditions are only observed in spring for MXEN. On the other hand, in CPEN events, the positioning of the subtropical jet at higher latitudes (around 40°S) is observed, which prevents precipitation in the Brazilian subtropical climate. These conditions are consistent with the precipitation anomalies found in this investigation (Figure 6) and are detailed in previous study [14].

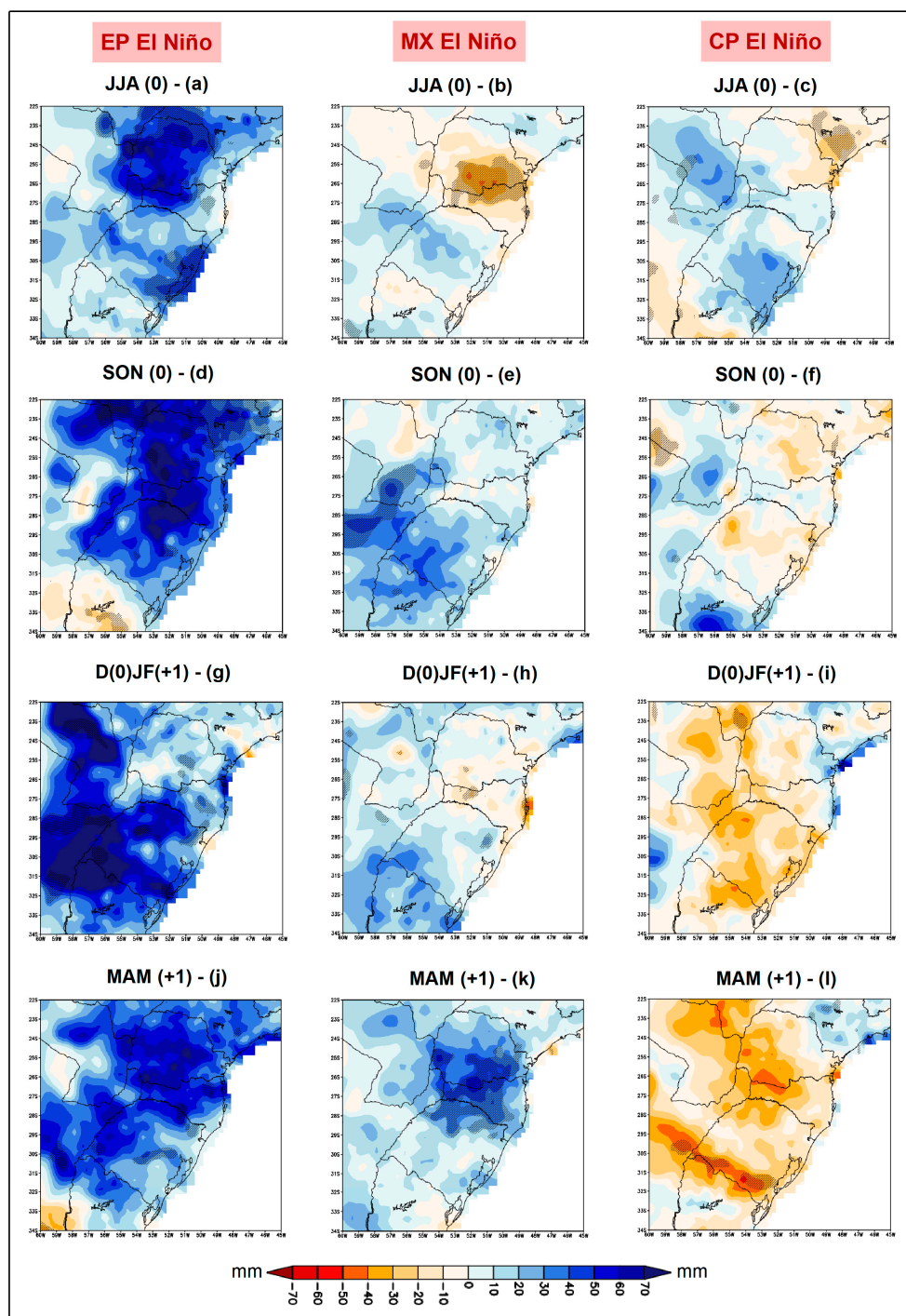


Figure 6. Composites of seasonal precipitation anomalies (1976 – 2019) in the Brazilian subtropical climate during different types of El Niño: East Pacific El Niño – EP El Niño (left column), Mixed El Niño – MX El Niño (middle column) and Central Pacific El Niño – CP El Niño (right column). (a,b,c) JJA (0); (d, e, f) SON (0); (g, h, i) D(0)JF(+1); and (j, k, l) MAM (+1). Hatched areas indicate statistical significance at the 90% confidence level.

Analyses previously developed for southeastern SA [14] demonstrated that, in EP-type events, the SALLJ, the subtropical jet stream (around 30°S – see supplementary material – Figure S1), and the Pacific-South America (PSA) pattern [44] are strengthened, and Rossby waves are better structured compared to CPEN. In CP-type events, these dynamics are especially displaced and weakened, which contributes to the configuration of negative rainfall anomalies in southern Brazil, particularly in MAM (+1) – Figure 6l. These results are also documented in other studies for SA [5,24,25,31,32,42].

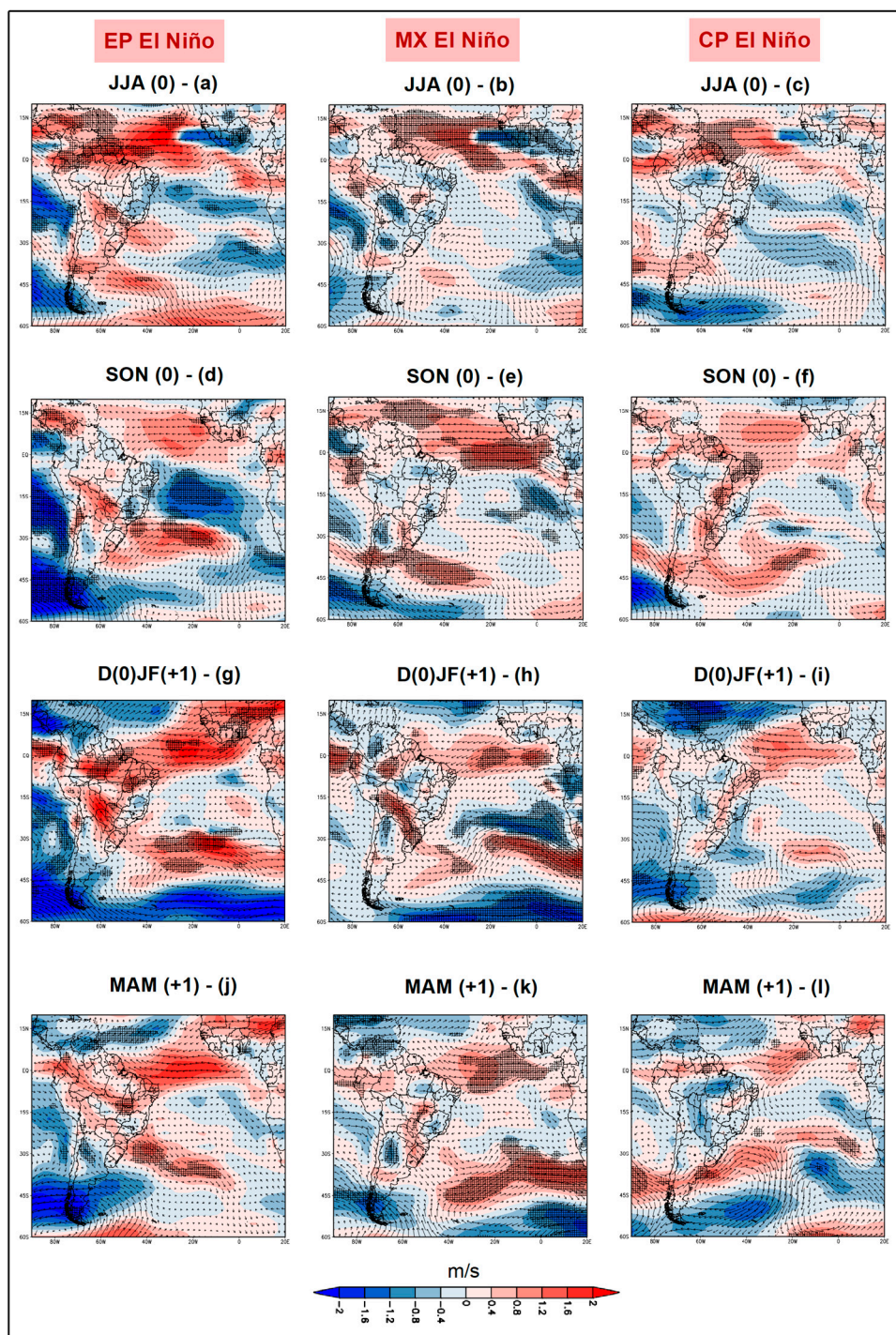


Figure 7. Composites of 850-hPa wind vector anomalies (m/s) over South America (1976 – 2019) during East Pacific El Niño – EP El Niño (left column), Mixed El Niño – MX El Niño (middle column) and Central Pacific El Niño – CP El Niño (right column). (a, b, c) JJA (0); (d, e, f) SON (0); (g, h, i) D(0)JF(+1); and (j, k, l) MAM (+1). Hatched areas indicate statistical significance at the 90% confidence level.

Regarding the LN-related rainfall patterns, the seasonal rainfall anomaly composites for EPLN (see Table 1) show larger negative precipitation anomalies in D(0)JF(+1) and MAM (+1) – Figures 8g and 8j. The most significant negative rainfall anomalies both in terms of spatial extent and magnitude occur in D(0)JF(+1), located mainly in the states of Paraná, Santa Catarina, and Rio Grande do Sul (Figure 8g). In this case, there is a weakening of the SALLJ-type circulation (Figure 9g), as well as a strengthening of the subtropical jet over the southeast SA (supplementary material – Figure S2).

Although the strengthening of the subtropical jet increases divergence in the upper levels, favoring the development or intensification of convective activity in the southeast of the SA, there was no increase in precipitation over southern Brazil (see Figure 8g). This configuration, associated with weak SALLJ-type circulation, reduces moisture transport at low levels from the Amazon region, limiting moisture convergence over the Brazilian subtropical region. As a result, despite favorable dynamic forces in the upper air, the vertical supply of moisture becomes insufficient to sustain deep convection or widespread precipitation. Therefore, rainfall events tend to be weaker.

The composites of seasonal precipitation anomalies for Mixed La Niña - MXLN (see Table 1) allows verifying that the most relevant negative precipitation anomalies occur in spring – SON (0), covering most of southern Brazil (Figure 8e). In MAM (+1), negative precipitation anomalies are observed along the border between Brazil (States of Paraná and Santa Catarina), Paraguay, and Argentina (Figure 8k). In both transitional seasons (SON and MAM), there is a marked weakening of the SALLJ-type circulation, as well as a strengthening of the subtropical jet stream. As in EPLN events in the Australian summer, there is dynamic support at high levels for the development of deep convection in southern Brazil, which was defavored by the weakening of the SALLJ-type circulation. In D(0)JF(+1), weak negative anomalies are concentrated in Rio Grande do Sul (Figure 8h), and in MAM (+1) along the border between Brazil (States of Paraná and Santa Catarina), Paraguay and Argentina (Figure 8k).

In the case of the composites of seasonal precipitation anomalies for CPLN (see Table 1), there are increases in precipitation in JJA (0), especially in the state of Paraná (Figure 8c) and decreases in the other seasons of the year (Figure 8f, Figure 8i, and Figure 8l). In SON (0), negative rainfall anomalies are concentrated in Rio Grande do Sul (Figure 8f). During the summer (D(0)JF(+1)), these dynamics shift to the western portion of the study area, with statistical significance only in Rio Grande do Sul (Figure 8i). In autumn (MAM+1), negative rainfall anomalies are located mainly in the northwest of Rio Grande do Sul and west of Santa Catarina and Paraná (Figure 8l).

Intense rainfall deficit occurs primarily in D(0)JF(+1) during EPLN (Figure 8g), and in SON (0) during MXLN (Figure 10e), while during CPLN, moderate rainfall deficit persists from SON (0) through MAM (+1) – Figures 8f, 8i and 8l. Thus, in the case of LN, variations are noted in terms of intensities of negative rainfall anomalies in the study area, contrary to what was found in EN, with changes in rainfall patterns between ENSO typologies (Figure 6).

Previous study [12] suggests that atmospheric circulation seems to be altered both by large-scale disturbances (changes in Walker and Hadley cells and Rossby waves) and by local factors (air temperature and soil humidity) that promote significant intraseasonal changes, especially in the austral summer. The differences in terms of negative rainfall anomalies between LN typologies result from changes in the Walker cell (during CPLN, Walker circulation anomalies in the central Pacific are stronger than during EPLN), the PSA pattern, and the strengthening (weakening) of the jets that transport more (less) moisture to southeast SA. These results are consistent with previous findings in the literature [5,24,31,32,42]. Higher frequency of SACZ events is also observed in LN years [45]. This fact reinforces the dipole pattern, with maximum precipitation over its southeast region and reductions in southern Brazil.

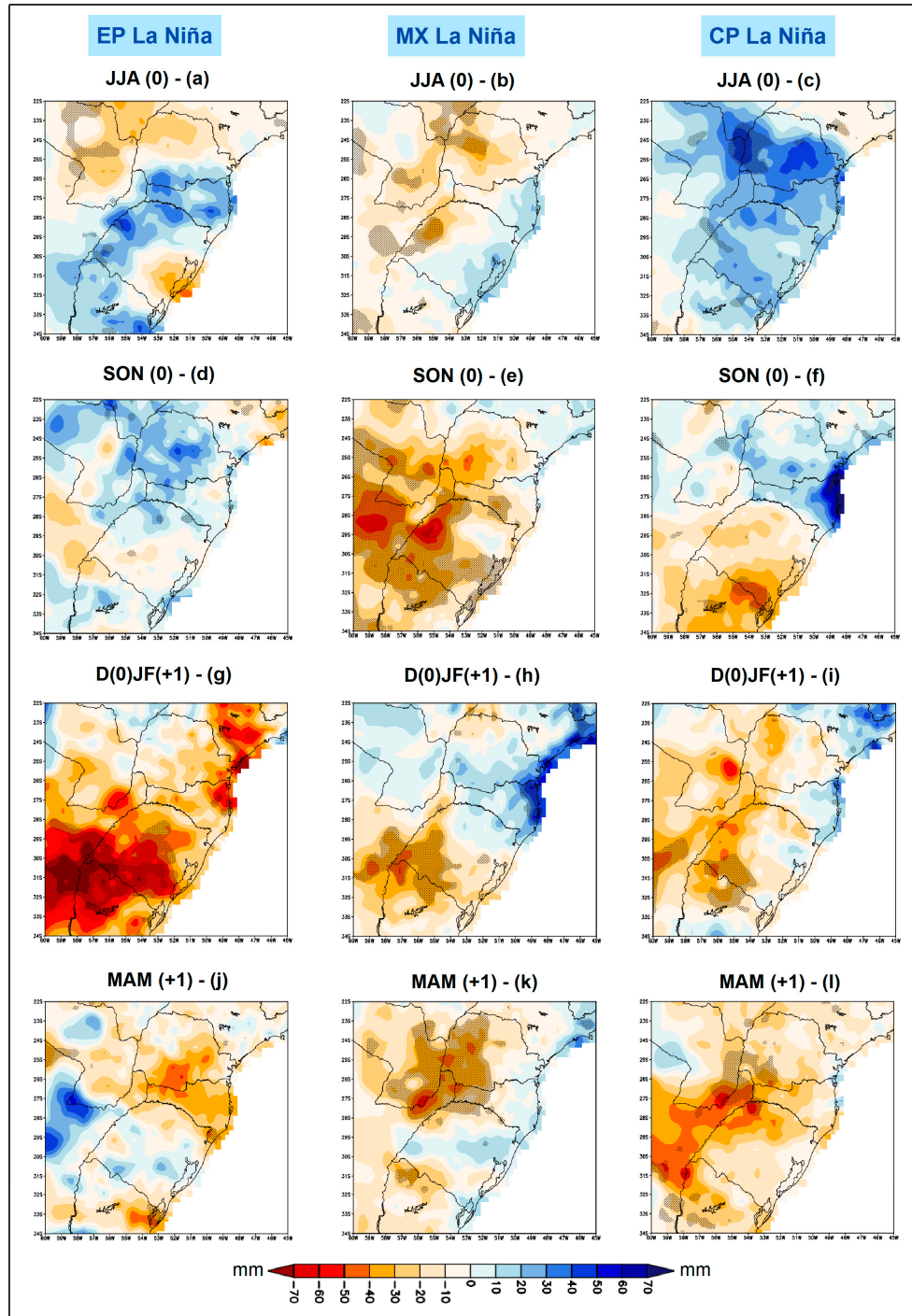


Figure 8. Composites of seasonal precipitation anomalies (1976 -2019) in the Brazilian subtropical climate during different types of La Niña: East Pacific La Niña – EP La Niña (left column), Mixed La Niña – MX La Niña (middle column) and Central Pacific La Niña – CP La Niña (right column). (a,b,c) JJA (0); (d, e, f) SON (0); (g, h, i) D(0)JF(+1); and (j, k, l) MAM (+1). Hatched areas indicate statistical significance at the 90% confidence level.

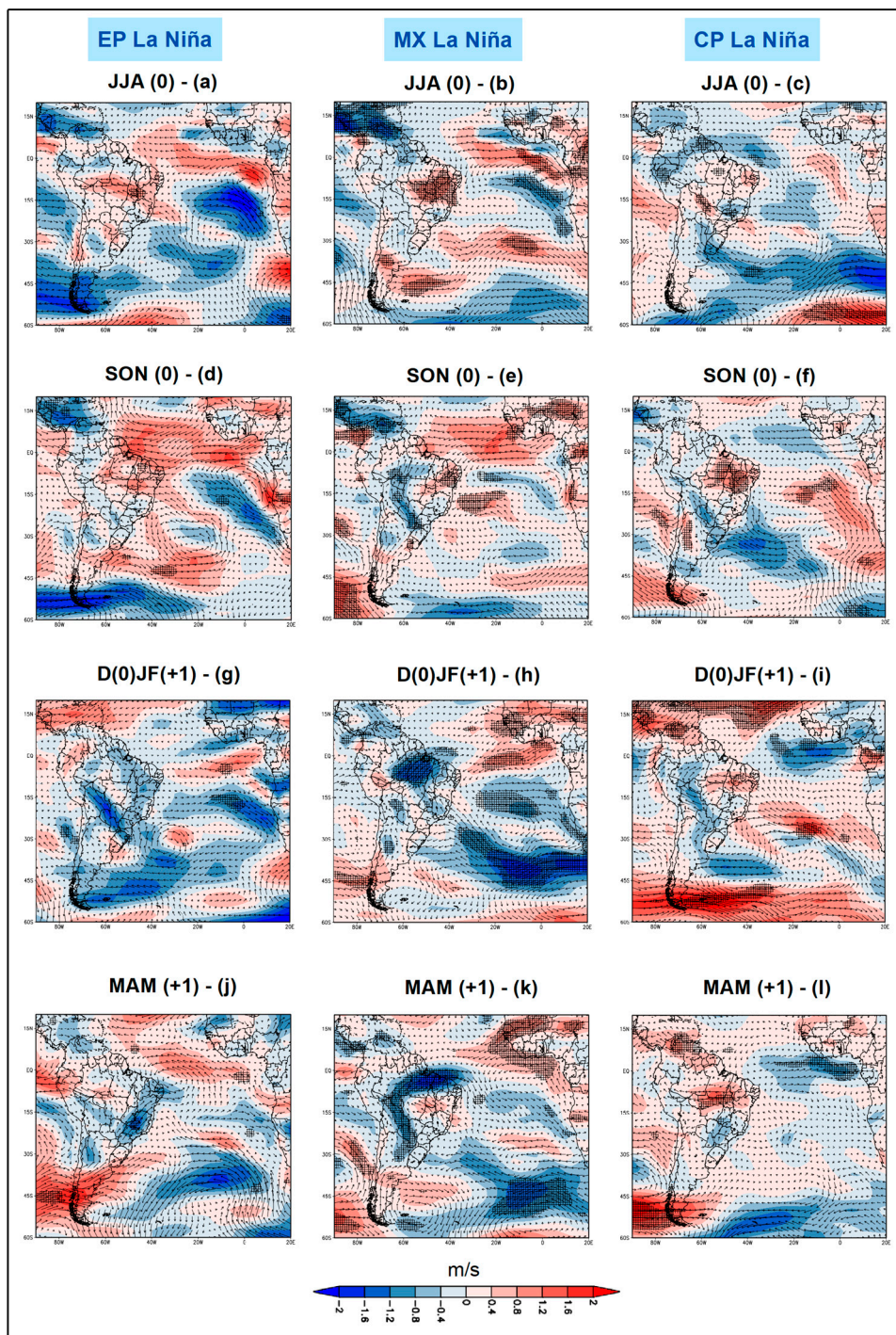


Figure 9. Composites of 850-hPa wind vector anomalies (m/s) over South America (1976 – 2019) during East Pacific La Niña – EP La Niña (left column), Mixed La Niña – MX La Niña (middle column), and Central Pacific La Niña – CP La Niña (right column). (a, b, c) JJA (0); (d, e, f) SON (0); (g, h, i) D(0)JF(+1); and (j, k, l) MAM (+1). Hatched areas indicate statistical significance at the 90% confidence level.

To better highlight precipitation variability and the effects of different ENSO types, the study area was divided into 9 homogeneous rainfall regions that reflect the rainfall diversity of the Brazilian subtropical climate (Figure 10). The regions with the highest rainfall totals are R3, R4, and R6, located along the coastal zone (R3 and R4) and in the western portion of the states of Paraná and Santa Catarina (R6), respectively. In these regions, mean annual precipitation totals reach 1735.4 mm, 2453.9 mm, and 1967.4 mm, respectively, based on the 1976 – 2019 climatology.

The regions located in the northern and eastern portions of the study area (R1, R2, R3, and R4) exhibit tropical climate characteristics, with enhanced precipitation during summer and marked decreases during winter. In contrast, the regions located in the southern portion of the study area (Rio Grande do Sul—R7, R8, and R9) are characterized by a more regular monthly distribution of rainfall.

The analysis of rainfall variations associated with different ENSO types in these regions (Figure 10) shows that strong EPEN years (1982–1983, 1997–1998, and 2015–2016—Table 1) were generally marked by positive rainfall anomalies across the homogeneous regions of the study area. Conversely, in some La Niña years (e.g., 1985, 2006, and 2018), a predominance of dry and extremely dry conditions was observed across most of the study regions.

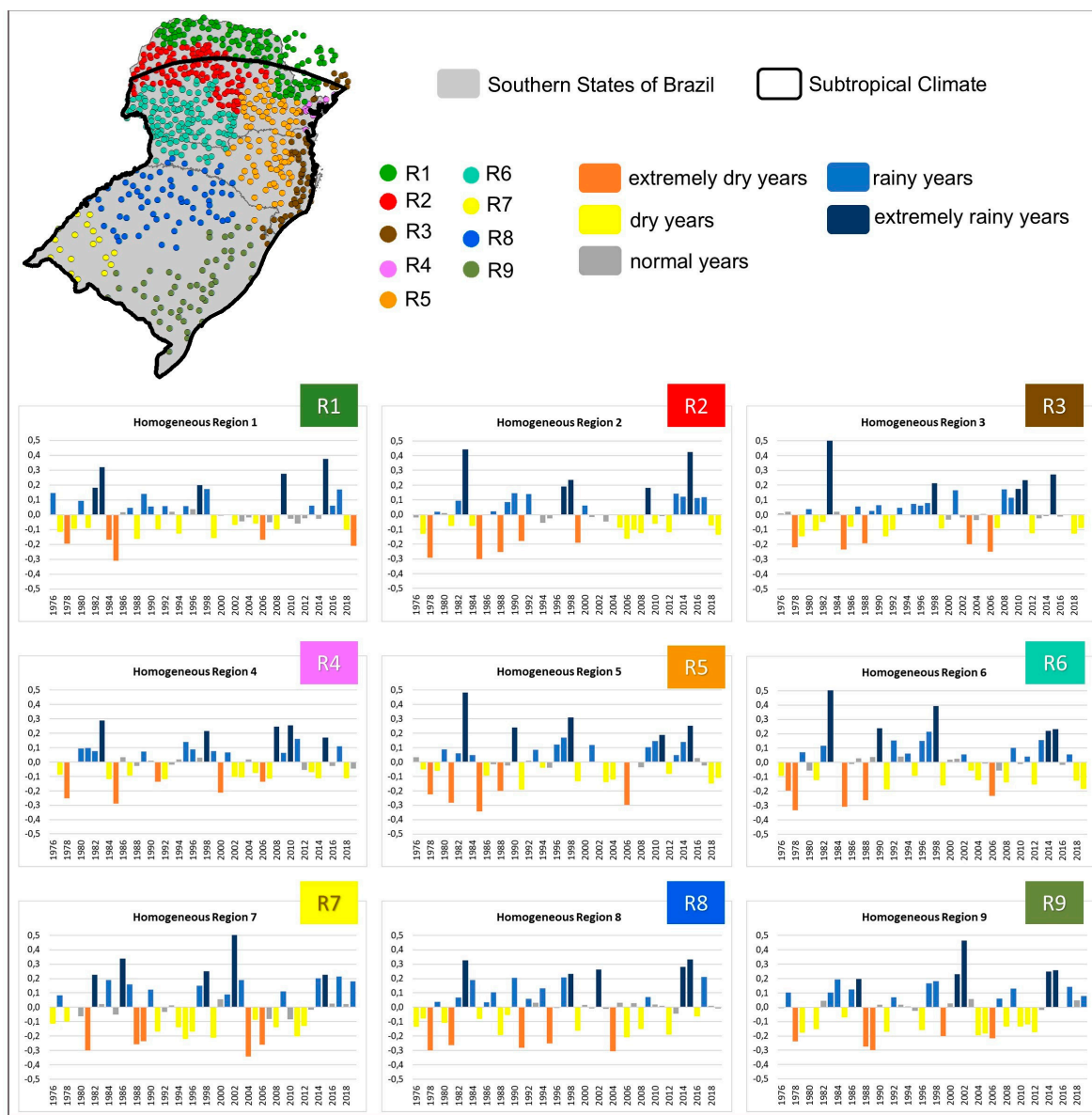


Figure 10. Coefficient of precipitation variation (-0.5 to 0.5) and classification of standard years by homogeneous rainfall regions in the Brazilian subtropical climate (1976 – 2019): extremely dry years (orange), dry years (yellow), normal years (gray), rainy years (light blue) and extremely rainy years (dark blue).

The years of strong EPEN intensity (1983, 1998, and 2015) were characterized as extremely rainy for the study area, with average annual variations of +603.4 mm (1983), +483.5 mm (2015), and +432.5 mm (1998), resulting in CVs of 50% variation in relation to the climatology from 1976 to 2019 (Figure 10). The most prominent regions were R6 and R3 (1983), R6 and R4 (1998), and R2 and R8 (2015).

In MXEN (Figure 10 and Table 1), greater variations between rainy and dry years are noted, with emphasis on 1988, with a predominance in the "extremely dry" classification in the study area, with average annual anomalies of -341.8 mm and emphasis on R6. In the CPEN (Figure 10 and Table 1), dry and extremely dry years predominate in the homogeneous regions defined in this study, with particular emphasis on the year 1978 (-428.9 mm annual average, especially in regions 6, 4, and 8).

The EPLN years (Figure 10 and Table 1) are characterized as extremely dry in most homogeneous regions. The years 1985 (average annual anomaly of -394.5 mm, with emphasis on R4 and R6), 2006 (average annual anomaly of -370.7 mm, with emphasis on R3, R5, and R6), and 2018 (average annual anomaly of -125.7 mm, with emphasis on regions R4, R6, R5 and R3) stand out.

In MXLN (Figure 10 and Table 1), greater variations in rainfall anomalies are observed, with the presence of both rainy and dry years in the homogeneous regions of this study. Dry and extremely dry years predominate in R7 and R9, while R4 was the region that presented the greatest variations (year 2000 with annual anomalies of -523.9 mm and 2008 with +600.3 mm). In the CPLN (Figure 10 and Table 1), variations in years with wetter (2001 and 2009) and drier (1999 and 2012) weather patterns were observed in the study area, with particular emphasis on R2, R6 and R7 (1999), R3 and R9 (2001), R1 and R2 (2009) and R6 and R8 (2012).

Overall, the rainfall variations in the homogeneous regions adopted in the present study reflect and corroborate the mappings in Figures 6 and 8. In EP-type El Niños, rainy and extremely rainy years predominate; in MXEN, greater variations between rainfall patterns are noted; and in CPEN, predominantly dry and extremely dry years stand out. Regarding LN, conventional patterns (EPLN) were characterized as dry and extremely dry, while MXLN and CPLN showed greater variations between homogeneous regions.

4. Conclusions

The main objective of this study was to analyze rainfall variability in the Brazilian subtropical climate associated with different ENSO typologies, considering both large-scale atmospheric mechanisms and regional rainfall behavior in homogeneous precipitation regions.

Previous studies have demonstrated that variations in ENSO typologies result from changes in the large-scale atmospheric circulation [5,11–14,25,31,32,42]. The results obtained in this study corroborate these mechanisms and demonstrate how they modulate rainfall variability in the Brazilian subtropical climate. This study advances previous analyses [14] by providing a refined regional assessment based on station-level data, reinforcing the importance of ENSO diversity for rainfall variability in the Brazilian subtropical climate.

By combining composite analyses of precipitation, wind fields, and SST anomalies with the assessment of homogeneous rainfall regions, this study provides a detailed regional perspective on the impacts of ENSO diversity. The findings reveal the magnitude and organization of rainfall anomalies depend strongly on ENSO typology, with EPEN events favoring extensive wet conditions and CPEN events producing more variable and, in some areas, opposite precipitation signals. MXEN events exhibit intermediate and more spatially heterogeneous rainfall patterns.

This regional-scale assessment demonstrates that ENSO diversity impacts are not spatially homogeneous within southeastern SA [14]. In the Brazilian subtropical climate, EPEN events produce more spatially coherent and statistically significant positive rainfall anomalies, particularly in SON (0) and DJF(+1), whereas CP events exhibit more heterogeneous patterns, with decreases in rainfall.

For LN, the results indicate a predominance of negative rainfall anomalies across most homogeneous regions, although the magnitude, spatial extent, and seasonal timing of these anomalies vary substantially among ENSO typologies. EPLN events are associated with the most intense summer rainfall deficits, while MX and CPLN events produce more variable and seasonally distinct dry conditions. These differences are closely linked to changes in the position and intensity of the SALLJ, the subtropical jet, and large-scale circulation patterns affecting moisture transport toward southern Brazil.

Overall, the results highlight the importance of considering ENSO diversity when assessing rainfall variability in the Brazilian subtropical climate and reveal asymmetric regional sensitivity to longitudinal SST shifts in the equatorial Pacific. Recognizing the distinct regional and seasonal impacts of ENSO typologies improves the understanding of climate variability and contributes to more accurate climate risk management and adaptation strategies in a region increasingly affected by both floods and droughts.

Supplementary Materials: The following supporting information can be downloaded at the website of this paper posted on Preprints.org. **Figure S1:** Composites of 200-hPa zonal wind anomaly (1976 – 2019) during East Pacific El Niño – EP El Niño (left column), Mixed El Niño – MX El Niño (middle column) and Central Pacific El Niño – CP El Niño (right column). (a, b, c) JJA (0). (d, e, f) SON (0). (g, h, i) D(0)JF(+1). (j, k, l) MAM (+1). Dotted areas show values with significance at the 90% level. **Figure S2:** Composites of 200-hPa zonal wind anomaly (1976 – 2019) during East Pacific La Niña – EP La Niña (left column), Mixed La Niña – MX La Niña (middle column) and Central Pacific La Niña – CP La Niña (right column). (a, b, c) JJA (0). (d, e, f) SON (0). (g, h, i) D(0)JF(+1). (j, k, l) MAM (+1). Dotted areas show values with significance at the 90% level.

Author Contributions: Conceptualization, G.G, L.L and F.M.; methodology, G.G, L.L and C.B.C; software, G.G. and C.B.C; validation, G.G.; formal analysis, G.G, L.L and C.B.C.; investigation, G.G.; data curation, G.G.; writing—original draft preparation, G.G.; writing—review and editing, G.G.; L.L, C.B.C and F.M; visualization, G.G.; L.L, C.B.C and F.M.; supervision, L.L and F.M.; project administration, F.M.; funding acquisition, F.M. All authors have read and agreed to the published version of the manuscript.

Funding: CAPES (Higher Education Personnel Improvement Coordination - Ministry of Education / Brazil) doctoral scholarship. NAPI Project - Climate Emergency. Funded by the Araucária Foundation - State of Paraná - Brazil. National Council for Scientific and Technological Development (CNPq, Brazil, Grant No. 440861/2023-3).

Institutional Review Board Statement: Not applicable.

Informed Consent Statement: Not applicable.

Data Availability Statement: Precipitation data from rainfall stations were made available by Hidroweb / National Water Agency, available at: <https://www.snirh.gov.br/hidroweb/serieshistoricas>. GPCC (GPCC Global Precipitation Climatology Centre) data were provided by Schneider *et al.* (2022) from the website at https://opendata.dwd.de/climate_environment/GPCC/html/fulldata-monthly_v2022_doi_download.html. NOAA Extended SST V5 (ERSST) were provided by the NOAA, Boulder, Colorado, USA, from their website at <https://psl.noaa.gov/data/gridded/data.noaa.ersst.v5.html> and ONI index data at https://origin.cpc.ncep.noaa.gov/products/analysis_monitoring/ensostuff/ONI_v5.php. Wind data were from NCEP/NCAR Reanalysis I (Kalnay *et al.*, 1996), available at: <https://psl.noaa.gov/data/gridded/data.ncep.reanalysis.html>.

Acknowledgments: The first author acknowledges CAPES (Higher Education Personnel Improvement Coordination - Ministry of Education / Brazil) for the financial support of the research in the form of a doctoral scholarship. We also thank the NAPI project - Climate Emergency, from the Araucaria do Paraná Foundation, for funding this article.

Conflicts of Interest: The authors declare no conflicts of interest.

Abbreviations

The following abbreviations are used in this manuscript:

CP	Central Pacific
CPEN	Central Pacific El Niño
CPLN	Central Pacific La Niña
EN	El Niño
ENSO	El Niño-Southern Oscillation

EP	East Pacific
EPEN	East Pacific El Niño
EPLN	East Pacific La Niña
LN	La Niña
MX	Mixed
MXEN	Mixed El Niño
MXLN	Mixed La Niña
PR	Paraná
RS	Rio Grande do Sul
SA	South America
SC	Santa Catarina

References

- Philander, S.G. *El Niño, La Niña and Southern Oscillation*. San Diego: Academic Press. 1990.
- Trenberth, K. E. The Definition of El Niño. *Bulletin of the American Meteorological Society*. 1997, 78, no. 12: 2771–2777. <https://doi.org/10.1175/1520-0477>
- McPhaden, M. J., S. E. Zebiak, and M. H. Glantz. ENSO as an Integrating Concept in Earth Science. *Science*, 2006, 314: 1740–1745. <https://doi.org/10.1126/science.1132588>
- Wang, C., Deser, C., Yu, J.-Y., Dinezio, P., Clement, A. El Niño – Southern Oscillation (ENSO): a review. In: Glynn, P.; Manzello, D.; Enochs, I (eds). *Coral reefs of the Eastern Pacific*. Springer Science Publisher, 2016, 85-106. https://doi.org/10.1007/978-94-017-7499-4_4
- Cai, W., McPhaden, M.J., Grimm, A.M., Rodrigues, R.R., Taschetto, A.S., Garreaud, R.D, *et al.* Climate impacts of the El Niño–Southern Oscillation on South America. *Nature Reviews Earth & Environment*. 2020, 1(4), 215-231. <https://doi.org/10.1038/s43017-020-0040-3>
- Goudard, G. *Interações oceano-atmosfera e efeitos na variabilidade pluvial do clima Subtropical brasileiro*. 323f. Tese (Doutorado em Geografia) - Pós-Graduação em Geografia, Setor de Ciências da Terra, Universidade Federal do Paraná, Curitiba. 2023.
- Reboita, M.S., Gan. M. A., da Rocha, S.P., Ambrizzi, T. Regimes de precipitação na América do Sul: uma revisão bibliográfica. *Revista Brasileira de Meteorologia*. 2010, v. 25, 185-204. <https://doi.org/10.1590/S0102-77862010000200004>
- Teixeira, M. D. S., Satyamurty, P. Trends in the frequency of intense precipitation events in southern and southeastern Brazil during 1960–2004. *Journal of climate*. 2011, 24(7), 1913-1921. <https://doi.org/10.1175/2011JCLI3511.1>
- Grimm, A.M. Clima da Região Sul. In: Cavalcanti, I.F.A; Ferreira, N.J. *Clima das regiões brasileiras e a variabilidade climática*. São Paulo: Oficina de Textos, 2021, p.70 – 84.
- Grimm, A.M., Ferraz, S.E.T., Gomes, J. Precipitation anomalies in Southern Brazil associated with El Niño and La Niña events. *Journal of Climate*. 1998, 11, n.10, 2863-2880. [https://doi.org/10.1175/1520-0442\(1998\)011<2863:PAISBA>2.0.CO;2](https://doi.org/10.1175/1520-0442(1998)011<2863:PAISBA>2.0.CO;2)
- Grimm, A.M. The El Niño impact on summer monsoon in Brazil: regional processes versus remote influences. *Journal of Climate*. 2003, 16: 263–280. [https://doi.org/10.1175/1520-0442\(2003\)016<0263:TENIOT>2.0.CO;2](https://doi.org/10.1175/1520-0442(2003)016<0263:TENIOT>2.0.CO;2)
- Grimm, A.M. How do La Niña events disturb the summer monsoon system in Brazil? *Climate Dynamics*. 2004, 22(2-3): 123–138. <https://doi.org/10.1007/s00382-003-0368-7>
- Grimm, A.M., Tedeschi, R.G. ENSO and extreme rainfall events in South America. *Journal of Climate*. 2009, 22: 1589–1609. <https://doi.org/10.1175/2008JCLI2429.1>
- Goudard, G., Limberger, L., Carpenedo, C. B. Influence of Eastern, Central and Mix El Niño on the variability of rainfall in southeastern South America. *Frontiers in Earth Science*. 2024, 12, 1134782. <https://doi.org/10.3389/feart.2024.1134782>
- Grimm, A. M., Almeida, A. S., Beneti, C. A. A., Leite, E. A. O efeito combinado de oscilações climáticas na produção de extremos: a seca de 2020 no Sul do Brasil. *Revista Brasileira de Recursos Hídricos – RBRH*. 2020, 25, e48. <https://doi.org/10.1590/2318-0331.252020200116>

16. Fernandes, V. R. *et al.* Secas e os impactos na região sul do Brasil. *Revista Brasileira de Climatologia*. 2021, 28, 561-584. <https://dx.doi.org/10.5380/rbclima.v28i0.74717>
17. Clarke, B *et al.* Climate change and El Niño behind extreme precipitation leading to major floods in southern Brazil in 2024. *npj Nat. Hazards*. 2026, 3, 4. <https://doi.org/10.1038/s44304-025-00162-8>
18. Du, H., *et al.* Precipitation from persistent extremes is increasing in most regions and globally. *Geophysical Research Letters*. 2019, 46(11), 6041-6049. <https://doi.org/10.1029/2019GL081898>
19. Regoto, P., Dereczynski, C., Chou, S. C., Bazzanella, A. C. Observed changes in air temperature and precipitation extremes over Brazil. *International Journal of Climatology*. 2021, 41(11), 5125-5142. <https://doi.org/10.1002/joc.7119>
20. Mamani, L., *et al.* The Cyclic and Episodic Transition of Strong El Niño and Implications for South American Precipitation During Their Peak and Decay Stages. *International Journal of Climatology*. 2024, 45(1), e8710. <https://doi.org/10.1002/joc.8710>
21. Tedeschi, R. G., Sampaio, G. Influences of different intensities of El Niño–Southern Oscillation on South American precipitation. *International Journal of Climatology*. 2022, 42(15), 7987-8007. <https://doi.org/10.1002/joc.7688>
22. Ashok, K., Behera, S.K., Rao, S.A., Weng, H.Y., Yamagata, T. El Niño Modoki and its possible teleconnection. *Journal of Geophysical Research*. 2007, 112: C11007. <https://doi.org/10.1029/2006JC003798>
23. Kao, H-Y, Yu J-Y. Contrasting eastern-Pacific and central-Pacific types of ENSO. *Journal of Climate*. 2009, 22, 615-632. <https://doi.org/10.1175/2008JCLI2309.1>
24. Andreoli, R.V, Oliveira, S.S, Kayano, M.T, Viegas, J., Souza, R.A.F, Candido, L.A. The influence of different El Niño types on the South American rainfall. *International Journal of Climatology* (published online). 2016, 37. [10.1002/joc.4783](https://doi.org/10.1002/joc.4783)
25. Kayano, M.T., Andreoli, R.V., Souza, R.A.F., Garcia, S.R., Calheiros, A.J. El Niño e La Niña dos últimos 30 anos: diferentes tipos. *Revista Climanalise. Edição Comemorativa*. 2016, 30. 7-12.
26. Wu, X., Okumura, Y. M., Dinezio, P. N. What controls the duration of El Niño and La Niña events?. *Journal of Climate*. 2019, 32(18), 5941-5965. <https://doi.org/10.1175/JCLI-D-18-0681.1>
27. Lin, J., Qian, T. Impacts of the ENSO lifecycle on stratospheric ozone and temperature. *Geophysical Research Letters*. 2019, 46(17-18), 10646-10658. <https://doi.org/10.1029/2019GL083697>
28. Kim, J. W., Yu, J. Y. Single-and multi-year ENSO events controlled by pantropical climate interactions. *Climate and Atmospheric Science*. 2022, 5(1), 88. <https://doi.org/10.1038/s41612-022-00305-y>
29. Li, X., Yu, J. Y., Ding, R. El Niño-La Niña asymmetries in the changes of ENSO complexities and dynamics since 1990. *Geophysical Research Letters*. 2024, 51(6), e2023GL106395. <https://doi.org/10.1029/2023GL106395>
30. Wang, B., *et al.* Historical change of El Niño properties sheds light on future changes of extreme El Niño. *Proceedings of the National Academy of Sciences*. 2019, 116(45), 22512-22517. <https://doi.org/10.1073/pnas.1911130116>
31. Tedeschi, R. G., Grimm, A. M., Cavalcanti, I. F. A. Influence of Central and East ENSO on extreme events of precipitation in South America during austral spring and summer. *International Journal of Climatology*. 2015, 35(8), 2045-2064. <https://doi.org/10.1002/joc.4106>
32. Tedeschi, R. G., Grimm, A. M., Cavalcanti, I. F. A. Influence of Central and East ENSO on precipitation and its extreme events in South America during austral autumn and winter. *International Journal of Climatology*. 2016, 36(15), 4797-4814. <https://doi.org/10.1002/joc.4670>
33. Costa, J. A. C., Andreoli, R. V., Kayano, M. T., de Souza, I. P., de Souza, R. A. F., Cerón, W. L. The South American precipitation trends under (or not) El Niño-Southern Oscillation influences and relationship with large-scale circulation. *International Journal of Climatology*. 2024, 44(9), 3154-3168. <https://doi.org/10.1002/joc.8518>
34. Schneider, U., Hänsel, S., Finger, P., Rustemeier, E., Ziese, M. *GPCC Full Data Monthly Product Version 2022 at 0.25°: Monthly Land-Surface Precipitation from Rain-Gauges built on GTS-based and Historical Data*. 2022, https://doi.org/10.5676/DWD_GPCC/FD_M_V2022_025
35. Huang, B., Thorne, P. W., Banzon, V. F., Boyer, T., Chepurin, G., Lawrimore, J. H. *et al.* Extended Reconstructed Sea Surface Temperature version 5 (ERSSTv5), Upgrades, validations, and intercomparisons. *Journal of Climate*. 2017, 30(20), 8179-8205. <https://doi.org/10.1175/JCLI-D-16-0836.1>

36. Kalnay, E. C., et al. The NMC/NCAR 40-year reanalysis project. *Bulletin of the American Meteorological Society*. 1996, 77(3), 437-472. Available at: <https://psl.noaa.gov/data/gridded/data.ncep.reanalysis.html>
37. Wold, H. Nonlinear iterative partial least squares (NIPALS) modelling: some current developments. In: *Multivariate analysis-III*. Academic Press. 1973, 383-407. <https://doi.org/10.1016/B978-0-12-426653-7.50032-6>
38. Wilks, D.S. *Statistical Methods in the Atmospheric Sciences*. 2^a ed. San Diego - CA: Elsevier. 2006.
39. Nascimento Junior, L. *As chuvas no Paraná: Variabilidade, teleconexões, e impactos de eventos extremos*. 162f. Dissertação (Mestrado em Geografia) - Universidade Estadual Paulista, Campus de Presidente Prudente, Presidente Prudente. 2013.
40. Yu, J., Kim, S. T. Identifying the types of major El Niño events since 1870. *International Journal of Climatology*. 2012, v. 33, n. 8, 2105-2112. <https://doi.org/10.1002/joc.3575>
41. Hill, K. J., Taschetto, A. S., England, M. H. Sensitivity of South American summer rainfall to tropical Pacific Ocean SST anomalies. *Geophysical Research Letters*. 2011, v. 38, n. 1. <https://doi.org/10.1029/2010GL045571>
42. Tedeschi, R. G. *As influências de tipos diferentes de ENOS na precipitação e nos seus eventos extremos sobre a América do Sul - observações, simulações e projeções*. 256f. Tese (Doutorado em Meteorologia) – Instituto Nacional de Pesquisas Espaciais, São José dos Campos. 2013.
43. Montini, T. L., Jones, C., Carvalho, L. M. The South American low-level jet: A new climatology, variability, and changes. *Journal of Geophysical Research: Atmospheres*. 2019, 124(3), 1200-1218. <https://doi.org/10.1029/2018JD029634>
44. Mo, K.C., Higgins, R.W. The Pacific–South American modes and tropical convection during the Southern Hemisphere winter. *Monthly Weather Review*. 1998, v. 126, n. 6, 1581-1596. [https://doi.org/10.1175/1520-0493\(1998\)126<1581:TPSAMA>2.0.CO;2](https://doi.org/10.1175/1520-0493(1998)126<1581:TPSAMA>2.0.CO;2)
45. Drumond, A. R. M., Ambrizzi, T. Inter ENSO variability and its influence over the South American monsoon system. *Advances in Geosciences*. 2006, v. 6, 167-171. <https://doi.org/10.5194/adgeo-6-167-2006>

Disclaimer/Publisher's Note: The statements, opinions and data contained in all publications are solely those of the individual author(s) and contributor(s) and not of MDPI and/or the editor(s). MDPI and/or the editor(s) disclaim responsibility for any injury to people or property resulting from any ideas, methods, instructions or products referred to in the content.